

This discussion paper is/has been under review for the journal *Climate of the Past* (CP).  
Please refer to the corresponding final paper in CP if available.

# Modeling the consequences on late Triassic environment of intense pulse-like degassing during the Central Atlantic Magmatic Province using the GEOCLIM model

G. Paris<sup>1,2</sup>, Y. Donnadiou<sup>3</sup>, V. Beaumont<sup>1</sup>, F. Fluteau<sup>2,4</sup>, and Y. Godd ris<sup>5</sup>

<sup>1</sup>Institut fran ais du p trole, 1 & 4 rue Bois-Pr au, 92 Rueil-Malmaison, France

<sup>2</sup>Institut de Physique du Globe, UMR7154, Sorbonne Paris Cit , 1 rue Jussieu, 75238 Paris cedex 05, France

<sup>3</sup>Laboratoires des Sciences du Climat de l'Environnement, CNRS-CEA, CEA Saclay, Orme des merisiers, B t. 701, 91191 Gif-sur-Yvette cedex, France

<sup>4</sup>UFR des Sciences de la Terre, de l'Environnement et des Plan tes, Universit  Paris 7, Sorbonne Paris Cit , 35 rue H l ne Brion, 75205 Paris cedex 13, France

<sup>5</sup>G osciences Environnement Toulouse, CNRS-Universit  de Toulouse III, 14 avenue E. Belin, 31400 Toulouse, France

## Modeling the consequences on late Triassic environment

G. Paris et al.

Title Page

Abstract

Introduction

Conclusions

References

Tables

Figures

⏪

⏩

◀

▶

Back

Close

Full Screen / Esc

Printer-friendly Version

Interactive Discussion

Received: 11 April 2012 – Accepted: 3 May 2012 – Published: 8 June 2012

Correspondence to: G. Paris (gparis@caltech.edu)

Published by Copernicus Publications on behalf of the European Geosciences Union.

CPD

8, 2075–2110, 2012

## Modeling the consequences on late Triassic environment

G. Paris et al.

Title Page

Abstract

Introduction

Conclusions

References

Tables

Figures



Back

Close

Full Screen / Esc

Printer-friendly Version

Interactive Discussion



## Abstract

The Triassic-Jurassic boundary (TJB) is associated with one of the five largest mass extinctions of the Phanerozoic. A deep carbon cycle perturbation and a carbonate production crisis are observed during the late Triassic. The Central Atlantic Magmatic Province (CAMP), one of the most important large igneous provinces of the Phanerozoic, emplaced at the TJB. To understand the carbon cycle perturbations observed at the TJB, we investigate the consequences of CO<sub>2</sub> degassing associated to the CAMP emplacement on atmospheric and oceanic carbon cycle. The CO<sub>2</sub> input within the atmosphere due to volcanism has been modeled using a global biogeochemical cycle box model (COMBINE) coupled with a climate model (FOAM). Weathering fluxes and CO<sub>2</sub> equilibrium are constrained by the Rhaetian paleogeography and different scenarios of the CAMP emplacement are modeled. The study focuses (1) on the geological record and the carbonate productions crisis and (2) on the sedimentary carbon isotope record. For point (1), comparison of different modeling scenarios shows that a Gaussian CO<sub>2</sub> emission distribution over the duration of the main activity phase of the CAMP fails in reproducing any of the geological observations, mainly the carbonate production crisis observed in the late Rhaetian sediments. Contrastingly, intense degassing peaks lead to successive decrease in carbonate production as observed in the geological record. For point (2), the perturbations of carbon cycle due to the degassing of CO<sub>2</sub> with a mantle carbon isotopic composition of  $-5\text{‰}$  do not reproduce the intensity of the observed carbon isotope excursions. This was achieved in our model by assuming a mantle carbon isotopic composition of  $-20\text{‰}$ . Even if this hypothesis requires further investigations, such low values may be associated to degassing of carbon from pools of light isotopic carbon located at the transition zone (Cartigny, 2010), possibly linked to setting of large igneous provinces (LIP's). Breakdown of biological primary productivity can also partially account for the sedimentary carbon isotope excursions and for the observed increase of atmospheric  $p\text{CO}_2$ .

## Modeling the consequences on late Triassic environment

G. Paris et al.

Title Page

Abstract

Introduction

Conclusions

References

Tables

Figures



Back

Close

Full Screen / Esc

Printer-friendly Version

Interactive Discussion



## 1 Introduction

The late Rhaetian is marked by one of the most important mass extinctions of the Phanerozoic, in both marine and terrestrial realms (Hesselbo et al., 2007; Sepkoski, 1996). The Triassic-Jurassic Boundary (TJB) crisis is interpreted as being the consequence of the Central Atlantic Magmatic Province (CAMP) emplacement, one of the most extended Large Igneous Province (LIP) of the Phanerozoic (Courtillot, 1994; Courtillot et al., 1999; Guex et al., 2004; McHone, 2002; Pálffy et al., 2001). The CAMP emplacement (Fig. 1) has affected atmospheric chemical composition due to degassing of CO<sub>2</sub> and sulfur gases (McElwain et al., 1999, 2009; McHone, 2002; Schaller et al., 2011). One of the most robust signals of the TJB crisis is the succession of two negative excursions in the records of the isotopic composition of sedimentary organic carbon ( $\delta^{13}\text{C}_{\text{org}}$ ), hereafter first and second excursions, respectively. The first excursion (Late Rhaetian) is associated with a negative excursion of the isotopic composition of mineral carbon ( $\delta^{13}\text{C}_{\text{min}}$ ), while this remains unclear for the second (early Hettangian) excursion. This isotopic pattern is recorded in worldwide sections spanning the late Rhaetian to early Hettangian (Galli et al., 2005; Guex et al., 2004; Hesselbo et al., 2002; Kürschner et al., 2007; Pálffy et al., 2001; Ruhl et al., 2009; Ward et al., 2001). The TJB crisis is also characterized by a late Rhaetian crisis of carbonate production and a perturbation of the biological pump in the Tethys seawater column (Kürschner et al., 2007; van de Schootbrugge et al., 2007, 2008; Clémence et al., 2010a,b; Paris et al., 2010).

General Circulation Models and carbon cycle models are a powerful tool to reconstruct carbon cycle perturbation in the past. Huynh and Poulsen (2005) used a coupled ocean–atmosphere climate model to explore the consequence of an atmospheric CO<sub>2</sub> increase on the late Rhaetian climate. They concluded that the Earth system would have been deeply perturbed by an increase of atmospheric CO<sub>2</sub>, with warm and dry summers affecting terrestrial ecosystems (Huynh and Poulsen, 2005). On the other hand, consequences of CO<sub>2</sub> degassing on oceanic carbon chemistry have been

CPD

8, 2075–2110, 2012

### Modeling the consequences on late Triassic environment

G. Paris et al.

Title Page

Abstract

Introduction

Conclusions

References

Tables

Figures

⏪

⏩

◀

▶

Back

Close

Full Screen / Esc

Printer-friendly Version

Interactive Discussion

## Modeling the consequences on late Triassic environment

G. Paris et al.

Title Page

Abstract

Introduction

Conclusions

References

Tables

Figures



Back

Close

Full Screen / Esc

Printer-friendly Version

Interactive Discussion



explored using the GEOCARB model (Beerling and Berner, 2002; Berner and Beerling, 2007). These authors suggested that the late Rhaetian negative  $\delta^{13}\text{C}$  excursion is due to clathrate dissociation (Beerling and Berner, 2002). They also concluded that the late Rhaetian carbonate production crisis was due to seawater undersaturation with respect to calcite, following  $\text{CO}_2$  and  $\text{SO}_2$  emission from the CAMP assuming both a very short duration of the CAMP emplacement (100 kyr) and a pre-crisis carbonate saturation state of 1.1.

Herein we want to re-explore the consequences of the  $\text{CO}_2$  emission from the CAMP with a different carbon cycle model and assuming different  $\text{CO}_2$  emission patterns according to recent paleomagnetic studies of CAMP volcanism. Indeed, degassing of  $\text{CO}_2$  from LIP is usually modeled as a Gaussian distribution over the duration of the eruption. It has been recently demonstrated that the CAMP emplacement occurred as a succession of intense and short-lived pulses (Knight et al., 2004). Consequences on the carbon cycle of such degassing scenarii are tested for the first time, in the specific paleoenvironmental context of the TJB.

The geochemical model, COMBINE used in this study, accounts for a rough spatialization of the sedimentary fluxes out of the ocean. This allows a realistic assessment of carbonate production. Indeed, at the TJB, most of the carbonate production occurs in epicontinental seas which are only a small part of the global ocean. Following the Knight et al. (2004) degassing model for the CAMP, we explore the consequences of atmospheric  $p\text{CO}_2$  variations on the production of carbonate in epicontinental seas. We then compare to the carbonate production perturbations obtained when using a Gaussian distribution of the degassing over the duration of the CAMP emplacement. Both degassing models are used to calculate the corresponding variations of sedimentary  $\delta^{13}\text{C}_{\text{org}}$  and  $\delta^{13}\text{C}_{\text{min}}$  signals. We also explore the consequences of an oceanic primary productivity shutdown on the carbon cycle and on the sedimentary carbon isotopic composition. Finally, we calculate the consequences of degassing isotopically light carbon (of  $-20\text{‰}$  rather than the canonical value of  $-5\text{‰}$ ) into the atmosphere.

Indeed, recent studies have highlighted the existence of such low isotopic carbon pools into the mantle.

## 2 Model description

### 2.1 General description

5 The GEOCLIM model (Donnadieu et al., 2006a) couples the FOAM general circulation model or GCM (Donnadieu et al., 2006b) to a model of the main biogeochemical cycles called COMBINE (Goddéris and Joachimski, 2004). The GCM is used to generate an offline catalogue of continental air temperature  $T_{\text{air}}$  and continental runoff  $R$  with a spatial resolution of  $7.5^\circ \text{ long} \times 4.5^\circ \text{ lat}$ . The atmospheric  $\text{CO}_2$  concentrations used  
10 in the FOAM simulations range from 200 ppm up to 4200 ppm, with an increment of 200 ppm. At each time step of the GEOCLIM calculation, and for each corresponding atmospheric  $p\text{CO}_2$ ,  $T_{\text{air}}$  and  $R$  above the continents are calculated through a linear interpolation procedure from the climatic catalogue. This procedure allows simultaneous calculation of climatic parameters and atmospheric  $p\text{CO}_2$ .

15 The ocean is longitudinally divided into three parts, two polar oceans and a low- to mid-latitude ocean (Fig. 2). Polar oceans are located between  $-90^\circ$  and  $-60^\circ$  latitude for the southern hemisphere and  $+60^\circ$  and  $+90^\circ$  latitude for the northern hemisphere. Each polar ocean includes a photic zone and a deep ocean reservoir. The low to mid latitude ocean is divided vertically into three parts that are a photic zone, a thermo-  
20 cline and a deep ocean reservoir. Two boxes representing epicontinental seas are also included, both with a photic zone and a deep epicontinental reservoir. A twelfth box represents the atmosphere. A full description of GEOCLIM and its components COMBINE and FOAM can be found in Goddéris and Joachimski (2004), Donnadieu et al. (2006a,b) and Simon et al. (2007). Key equations describing fluxes are given in  
25 Table 2.

## Modeling the consequences on late Triassic environment

G. Paris et al.

Title Page

Abstract

Introduction

Conclusions

References

Tables

Figures

⏪

⏩

◀

▶

Back

Close

Full Screen / Esc

Printer-friendly Version

Interactive Discussion



## 2.2 Weathering fluxes and CO<sub>2</sub> consumption

The model describes the biogeochemical cycles for carbon, phosphorus, alkalinity and oxygen. The steady state  $p\text{CO}_2$  is defined by the volcanic degassing and the total continental silicate weathering (that is the sum of the weathering in each continental cell) at the used continental configuration. Based on recent works suggesting a constant oceanic production crust rate for the last 180 Ma (Rowley, 2002), the CO<sub>2</sub> degassing background value is set to the modern one; ie.  $6.8 \times 10^{12} \text{ mol C yr}^{-1}$ . This value is chosen to balance present day net global CO<sub>2</sub> consumption through silicate weathering after carbonate precipitation in the ocean. The total silicate weathering flux is  $13.6 \times 10^{12}$  moles of atmospheric CO<sub>2</sub> yr<sup>-1</sup> for present day (Gaillardet et al., 1999) and  $k_{\text{silw}}$  and  $k_{\text{basw}}$  constants are calibrated using a present day control FOAM climatic simulation, assuming that 30 % of the total atmospheric CO<sub>2</sub> consumption by silicate weathering is due to basalt weathering (Dessert et al., 2003). The calibration constant for phosphate weathering  $k_{\text{pw}}$  is set so that the modern flux  $F_{\text{pw}}$  equals  $45 \times 10^9 \text{ mol yr}^{-1}$  (Donnadieu et al., 2006). Although continental weathering fluxes are spatially resolved, the model does not account for a variation in the spatial distribution of lithologies. All lithological types are assumed to be present in the same proportion over each continental grid cell (see Donnadieu et al., 2006 for more details).

## 2.3 Carbonate formation and deposition

Accumulation of neritic carbonates on shelves and accumulation of pelagic carbonates on the seafloor are calculated in the model. No constraint is set on the total deposition flux that adapts until the alkalinity removed through deposition and the alkalinity added from continental weathering balance each other. The shelf platform area is thought to have been larger in the past and is set to be 18 times larger than the modern one in our study (Walker et al., 2002). The calibration constant for reef carbonate accumulation  $k_{\text{cr}}$  is calibrated so that the present day deep sea carbonate

CPD

8, 2075–2110, 2012

### Modeling the consequences on late Triassic environment

G. Paris et al.

Title Page

Abstract

Introduction

Conclusions

References

Tables

Figures

⏪

⏩

◀

▶

Back

Close

Full Screen / Esc

Printer-friendly Version

Interactive Discussion



estimate the consequences of CAMP emplacement on late Rhaetian carbon cycle, we establish degassing scenarios, based on geological, geochemical and paleomagnetic studies of the CAMP.

### 3.1 Duration

5 The CAMP consists in floods, sills and dykes outcropping in Africa, South and North America and Meridional Europe (Marzoli et al., 1999; Prévot and McWilliams, 1989). The CAMP total surface is estimated at  $2\text{--}6 \times 10^6 \text{ km}^2$  with a flood mean thickness of 150–300 m (Marzoli et al., 1999). The duration of the CAMP paroxysmal activity phase was estimated at  $580 \pm 100 \text{ kyr}$  using magnetostratigraphy and cyclostratigraphy (Olsen et al., 1996). The duration was confirmed by Nomade et al. (2007) using  $^{40}\text{Ar}/^{39}\text{Ar}$  ages. Hesselbo et al. (2002) have found the first  $\delta^{13}\text{C}$  negative excursion in a T-J marine section from UK and a terrestrial section from Greenland together. The first  $\delta^{13}\text{C}$  negative excursion has been estimated to last between less than 200 ky and 500 ky (Guex et al., 2004; Schoene et al., 2010; Ward et al., 2001) and is interpreted as occurring during the CAMP volcanism (Fig. 1). Indeed Schoene et al. (2010) suggest that the first negative excursion is concomitant to the emplacement of North Mountain basalt formation (NMB, Fundy basin), itself contemporaneous to the Orange Mountain basalt formation (OMB, Newark basin). Observation and geochemical evidences (Marzoli et al., 2004) indicate that a portion of the intermediate unit and the entire lower unit are absent in the Newark Basin (Fig. 1). Thus a significant part of CAMP could be erupted before the emplacement of these units (Cirilli et al., 2009; Knight et al., 2004; Marzoli et al., 2004), and, as a consequence, prior to the first excursion. The total duration is estimated at 500 kyr, in agreement with the estimated duration of the CAMP paroxysmal activity (Marzoli et al., 1999; Olsen et al., 1996; Schoene et al., 2010).

## Modeling the consequences on late Triassic environment

G. Paris et al.

Title Page

Abstract

Introduction

Conclusions

References

Tables

Figures

⏪

⏩

◀

▶

Back

Close

Full Screen / Esc

Printer-friendly Version

Interactive Discussion



## 3.2 Degassing pattern

CAMP was erupted in several major phases separated by periods of volcanic quiescence allowing the deposition of sediments. A close-up reveals that each volcanic phase consists in the emplacement of successive lava flows. Isotopic dating yielded ages with uncertainties, which remain by far too large to determine the tempo of the emplacement of the volcanic pile (Knight et al., 2004). To overcome this difficulty, a relative chronometer using the secular variation of the Earth magnetic field has been developed (Mankinen et al., 1985). Superimposed lava flows of LIPs provide a suite of snapshot of the Earth magnetic field recorded during the cooling of lava (Mankinen et al., 1985; Riisager et al., 2002, 2003; Knight et al., 2004; Chenet et al., 2008, 2009; Moulin et al., 2011). Several successive lava flows can display statistically indistinguishable paleomagnetic directions revealing that this group of lava flows (also called volcanic pulse) were erupted over a period likely shorter than 400 yr (Knight et al., 2004), or perhaps as short as a century or even less for the Deccan traps (Chenet et al., 2008, 2009; Moulin et al., 2011). Knight et al. (2004) applied this method on a section sampled in Morocco to determine the tempo of volcanism. This section is divided into a Lower Unit, an Intermediate Unit and an Upper Unit according geochemical data and changes in flow texture. Each unit consists in a pile of superimposed lava flows with occasionally intertrappean sedimentary layers. Based on the analyses of magnetic directions, Knight et al. (2004) recognized within the 3 volcanic units, 5 volcanic pulses erupting large amounts of basalt ( $\sim 10^4 \text{ km}^3$  each) and one single lava flow. Because the North African part of CAMP was partly formed earlier than that of North America, we chose to represent the whole CAMP eruption as ten identical volcanic pulses equally spaced in time rather than considering three pulses only as described by Schaller et al. (2011) or six as described by Knight et al. (2004).

### Modeling the consequences on late Triassic environment

G. Paris et al.

Title Page

Abstract

Introduction

Conclusions

References

Tables

Figures



Back

Close

Full Screen / Esc

Printer-friendly Version

Interactive Discussion



### 3.3 Volume of degassed CO<sub>2</sub>

The volume of CO<sub>2</sub> likely released during CAMP emplacement is bracketed by a “low” and a “high” hypothesis (Table 1). The first (“low hypothesis”) corresponds to a total volume of 1400 Gt C (McHone, 2002). The second one (“high hypothesis”) corresponds to the CO<sub>2</sub> that would be degassed by the highest possible estimated basalt volume of the CAMP, including not only outcrops and seaward dipping reflectors from eastern USA but also a volume of intrusive CAMP rocks doubling roughly this total amount (Beerling and Berner, 2002). The CO<sub>2</sub> release is calculated using a CO<sub>2</sub> content of 0.6 % wt in the magma and a 100 % degassing. Total CO<sub>2</sub> emissions then reach 34 900 Gt C. The discussion will be oriented towards the hypothesis of an emitted CO<sub>2</sub> amount similar to the one used by Berner and Beerling (2007), 21 200 Gt C or 77 700 Gt CO<sub>2</sub>. This is roughly twice the total amount of CO<sub>2</sub> (33 600 Gt CO<sub>2</sub>) suggested by Schaller et al. (2011) but this setting allows a comparison with previous modeling studies.

### 3.4 Degassing scenarii used for modeling

The degassing from LIP basalt flooding is usually modeled as a Gaussian distribution or a step function spanning the trap emplacement (Beerling and Berner, 2002; Dessert et al., 2001; Grard et al., 2005). To test the potential role played by the CAMP in the TJB mass extinction, two different degassing scenarios have been modeled (Fig. 3). The first one (A) is represented by a Gaussian degassing over 500 kyr. The second one (B) consists in a succession of ten identical pulses lasting 100 yr each and uniformly distributed over 500 kyr. Each of these peaks represents then 2100 Gt C or 6300 Gt CO<sub>2</sub>, half the 11 000 Gt CO<sub>2</sub> peaks for each of the three pulses evaluated by Schaller et al. (2011, Fig. 3a). Two different degassing patterns are tested, with same duration and total amount of degassed CO<sub>2</sub> (21 000 Gt C).

## Modeling the consequences on late Triassic environment

G. Paris et al.

Title Page

Abstract

Introduction

Conclusions

References

Tables

Figures

⏪

⏩

◀

▶

Back

Close

Full Screen / Esc

Printer-friendly Version

Interactive Discussion



## 4 Parameters of the carbon system

### DIC and alkalinity

The results of the model will first be described in terms of carbon partition in the different reservoirs. In the case A (Gaussian degassing), CO<sub>2</sub> emissions from the CAMP are mostly buffered by the ocean, limiting atmospheric pCO<sub>2</sub> increase and average saturation state and pH decrease in the global ocean, from 2.15 to 1.65 and by 0.25 pH unit, respectively. In epicontinental seas, pH decreases by 0.2 units while alkalinity and DIC (Dissolved Inorganic Carbon) increase (resp. from 2.6 to 4 mmol kg<sup>-1</sup> and 2.65 to 3.85 mmol kg<sup>-1</sup>). Contrasted responses are observed depending on the considered part of the modeled ocean. The alkalinity increase is due to warming following the atmospheric CO<sub>2</sub> increase, enhancing continental weathering, counteracting for the ocean acidification due to CO<sub>2</sub> increase. This leads, in the model, to favorable conditions for reef carbonate production (increase of the saturation state), which increases from 22 × 10<sup>12</sup> to 31 × 10<sup>12</sup> mol C yr<sup>-1</sup> (Fig. 4). Organic matter sedimentation increases from 3.5 × 10<sup>12</sup> to 4.7 × 10<sup>12</sup> mol C yr<sup>-1</sup> and pelagic carbonate production from 3.4 × 10<sup>12</sup> to 4.4 × 10<sup>12</sup> mol C yr<sup>-1</sup>, generating a storage of carbon out of the ocean-atmosphere system.

In case B (pulse degassing), concomitant to each pulse, the CO<sub>2</sub> ocean uptake flux is reversed from an equilibrium flux of 13 × 10<sup>12</sup> mol C yr<sup>-1</sup> from the atmosphere to the ocean to 150 × 10<sup>12</sup> mol C yr<sup>-1</sup> from the ocean to the atmosphere likely due to fast ocean acidification generating a release of CO<sub>2</sub> by the ocean. Variations of the ocean-atmosphere exchange fluxes constitute the most striking difference simulated between scenarios A and B. The ocean can not absorb CO<sub>2</sub> because the emission rate is too large during the pulses. Short term peaks of 750 ppm atmospheric pCO<sub>2</sub> increase (Fig. 3c) are associated with short term decreases by 0.15 pH units in the world ocean (and in epicontinental seas) associated to saturation state decrease (Fig. 4). This leads to a succession of dropdowns in neritic carbonate production (decrease of 7.5 × 10<sup>12</sup> mol C yr<sup>-1</sup>, i.e. 30%), yet stacked on a long-term increase of the reef

## Modeling the consequences on late Triassic environment

G. Paris et al.

Title Page

Abstract

Introduction

Conclusions

References

Tables

Figures

⏪

⏩

◀

▶

Back

Close

Full Screen / Esc

Printer-friendly Version

Interactive Discussion



production flux from  $22 \times 10^{12}$  to  $26 \times 10^{12}$  mol C yr<sup>-1</sup> due to the overall increase in alkalinity following enhanced weathering. On the other hand, primary production seems to be favored by these peaks of CO<sub>2</sub> emission. The calcareous pelagic production being calculated to be proportional to global primary production, the modeled pelagic carbonate production is marked by short term increases of  $0.5 \times 10^{12}$  mol C yr<sup>-1</sup> and long term increase of  $3.4 \times 10^{12}$  to  $4.2 \times 10^{12}$  mol C yr<sup>-1</sup>, thus generating a different response compared to the reef production one.

## 5 Carbon isotopic signals

### 5.1 Isotopic fractionation due to atmospheric $p\text{CO}_2$ increase

The CO<sub>2</sub> degassing impact on  $\delta^{13}\text{C}$  in case A and B is shown for the atmospheric reservoir, organic matter and carbonates produced in the photic zone of the epicontinental sea (Fig. 5). Global trends are similar for both scenarios. Atmosphere and OM are affected by a decrease of the  $\delta^{13}\text{C}$  values, more intense with the Gaussian scenario (case A, -3‰ in OM and -2‰ for atmospheric carbon) than the pulse scenario (case B). The total duration of the negative excursion is longer for the scenario B. The 3‰  $\delta^{13}\text{C}_{\text{org}}$  negative excursion simulated in the case A where  $\varepsilon_p$  is  $p\text{CO}_2$  dependent (Eq. 1) is of the same order than the -4 to -6 ‰ excursion observed in late Rhaetian organic sediments. However, the tested scenario fails in reproducing the totality of negative isotopic excursion recorded in TJB sediments.

### 5.2 Isotopic composition of the emitted CO<sub>2</sub>

The isotopic composition of carbon emitted by the CAMP used in this model is -5‰. However Deines (2002) established the existence of a minor pool of light mantellic carbon ( $\delta^{13}\text{C}$  values from -22‰ to -26‰), which was observed in the dissolution residue of mantle minerals (olivine, pyroxene) and rocks, and thought to be indigenous to the

CPD

8, 2075–2110, 2012

## Modeling the consequences on late Triassic environment

G. Paris et al.

Title Page

Abstract

Introduction

Conclusions

References

Tables

Figures

◀

▶

◀

▶

Back

Close

Full Screen / Esc

Printer-friendly Version

Interactive Discussion



## Modeling the consequences on late Triassic environment

G. Paris et al.

[Title Page](#)

[Abstract](#)

[Introduction](#)

[Conclusions](#)

[References](#)

[Tables](#)

[Figures](#)

[⏪](#)

[⏩](#)

[◀](#)

[▶](#)

[Back](#)

[Close](#)

[Full Screen / Esc](#)

[Printer-friendly Version](#)

[Interactive Discussion](#)



5 mantle based on data from various xenoliths. Deines (2002) explicitly rejected the possibility of secondary contamination of the samples by organic carbon. The  $\delta^{13}\text{C}$  analysis of xenoliths from basalts highlighted a bimodal distribution with two main peaks at  $-5\text{‰}$  and  $-25\text{‰}$  although the geologic occurrence of this light carbon has not been clearly delineated (Deines, 2002). This is the case for xenoliths from both hotspot and non-hotspot volcanoes and xenoliths from kimberlites. According to Deines (2002), the light  $\delta^{13}\text{C}$  signatures are consistent neither with assumed limited indigenous carbon isotope variability within the mantle, nor with the supposition that all  $^{13}\text{C}$  depleted carbon are of surface origin. Such a bimodal  $\delta^{13}\text{C}$  distribution is not as obvious in diamond  $\delta^{13}\text{C}$  values only (Cartigny, 2005). However, the  $\delta^{13}\text{C}$  distributions of the peridotitic and eclogitic diamonds are significantly different. The range is narrower for peridotitic diamonds ( $\delta^{13}\text{C}$  values from  $-26.4$  to  $+0.2\text{‰}$ ) compared to eclogitic diamonds  $\delta^{13}\text{C}$ , from  $-38.5$  to  $+2.7\text{‰}$  (Cartigny, 2005). These values can be due to either distinct carbon source or primordial variability or isotope fractionation at mantle temperature, the first hypothesis being the favored one (Cartigny, 2005). A more recent study exhibits diamonds from the Dachine komatiite with characteristics very close to the carbonados (diamonds with  $\delta^{13}\text{C}$  of ca.  $-25\text{‰}$ ) the latter being sometimes interpreted as extra-terrestrial in origin, suggesting a possible mantellic origin of such light isotopic composition (Cartigny, 2010). This study suggests the existence of pools with carbon depleted in  $^{13}\text{C}$  at the transition zone. The origin of the CAMP tholeiitic series seems to be rooted in the lithosphere (McHone, 2000) but ultimately linked to the ascent of the Central Atlantic plume at the base of the lithosphere and later lithospheric contamination. However, pools of light isotopic carbon seem to exist in the mantle, with unclear origin and/or location. A degassed  $\text{CO}_2$  with a carbon isotopic composition of  $-20\text{‰}$  appears nevertheless as a relevant modeling hypothesis, acknowledging that all or only part of the degassing  $\text{CO}_2$  could be concerned by this low isotopic signature. We test the consequences of such light degassed carbon on the late Rhaetian carbon cycle (Fig. 6). If the  $\delta^{13}\text{C}_{\text{CO}_2}$  value is set to  $-20\text{‰}$ , the intensity of the modeled CIE (carbon isotopic excursion) is closer to the sedimentary geochemical signal. The

isotopic composition of OM is the most significantly affected, with a  $-6\%$  negative excursion, while the isotopic composition of the atmosphere is lowered by  $-2.5\%$  and that of the carbonates by  $-3\%$ . The results fit to the sedimentary records, the  $^{12}\text{C}$  enrichment being more pronounced in OM than in carbonates. This difference of intensity could be explained by the increase of fractionation related to the increase of atmospheric  $p\text{CO}_2$  (Eq. 1) and, to a lesser extent by the difference of intensity of the flux (carbonate deposition flux is one order of magnitude bigger than the OM deposition flux).

### 5.3 Consequences of oceanic primary productivity shutdown

Drastic perturbation of the biological production can have a large effect on carbon isotopic shift. In our model, the CAMP  $\text{CO}_2$  degassing induces an increase in the biological production. This is due to the atmospheric  $p\text{CO}_2$  increase and coeval increase of weathering and phosphorus delivery flux, promoting bioproductivity in the ocean. This is not consistent with data suggesting a decrease in primary production across the TJB. In order to test the influence of primary production crisis on the isotopic composition of the carbon reservoirs, we force a dropdown of the biological activity.

A total shutdown of the oceanic primary productivity is unlikely to have occurred during the late Rhaetian event but is used as an extreme hypothesis to explore the consequences on the isotopic composition of the sedimentary carbon across the TJB, independently from any CAMP degassing. Thus, we forced the production to stop for (1) 50 kyr and (2) 500 kyr in order to test the influence of primary production on the  $\delta^{13}\text{C}_{\text{org}}$  signal (Fig. 7). In both cases, the shutdown is set to occur instantaneously while the recovery is exponentially defined so that the primary production level reaches 2/3 of its pre-crisis intensity within 100 kyr. In the 50 kyr case, the atmospheric  $\text{CO}_2$  concentration increases by 200 ppm only as oceanic productivity stops and in the 500 kyr case, the atmospheric  $p\text{CO}_2$  increases from its background level to 2200 ppm.

The phase of biological productivity shutdown itself generates a  $+5\%$  excursion in  $\delta^{13}\text{C}_{\text{org}}$  signal. This signal can not be extensively interpreted insofar as virtually no

## Modeling the consequences on late Triassic environment

G. Paris et al.

Title Page

Abstract

Introduction

Conclusions

References

Tables

Figures

⏪

⏩

◀

▶

Back

Close

Full Screen / Esc

Printer-friendly Version

Interactive Discussion



oceanic organic matter is produced according to our scenario. However, these  $\delta^{13}\text{C}_{\text{org}}$  excursions are likely explained by the much lower uptake of  $^{12}\text{C}$  by a strongly decreased primary production. Both atmosphere and carbonates  $\delta^{13}\text{C}$  compositions decrease by 1‰. In the 500 kyr scenario, the negative excursions in atmosphere and carbonates  $\delta^{13}\text{C}$  values last as long as the productivity is stopped.

As soon as productivity starts to recover,  $\delta^{13}\text{C}_{\text{org}}$  values decrease, due to  $\text{CO}_2$  concentration increase that maximizes the isotopic fractionation between  $\text{CO}_2$  and biological organic matter. This counteracts for the phosphate accumulation and likely lowers isotopic composition of seawater itself due to  $^{12}\text{C}$  relative accumulation. Recovery of oceanic bioproductivity is associated to a negative excursion in  $\delta^{13}\text{C}_{\text{org}}$  values in both cases, but in the 50 kyr scenario, the amplitude is modest (0.5‰) while a  $-2\%$  negative excursion is observed in the 500 kyr scenario. According to the present model, even an almost complete shutdown of the primary production is not sufficient in itself to reproduce the intensity of the observed first excursion (late Rhaetian) in the  $\delta^{13}\text{C}_{\text{org}}$  signal.

## 6 Discussion

Computing the biological response to volcanic emissions is a challenging issue. We can not predict continental biosphere response to our scenario, such as direct biomass poisoning or burning by basalt flooding as previously suggested (van de Schootbrugge et al., 2009). CAMP emissions are suspected to have contained  $\text{SO}_2$  and dusts, generating aerosols, enhancing seawater acidification and atmosphere darkening (McHone, 2002; Guex et al., 2005). There is also an impact on the continental weathering flux due to dissolved sulfuric acid (Li et al., 2008). In such a case, continental carbonate dissolution acts as a positive feedback on atmospheric  $p\text{CO}_2$ , releasing carbon in the ocean-atmosphere system. These parameters are not taken into account in the model,

## Modeling the consequences on late Triassic environment

G. Paris et al.

Title Page

Abstract

Introduction

Conclusions

References

Tables

Figures

⏪

⏩

◀

▶

Back

Close

Full Screen / Esc

Printer-friendly Version

Interactive Discussion



because of the lack of constraints on the flux and their consequences on the carbon cycle.

One of the remaining questions about our results is the pelagic carbonate productivity response to the degassing scenario of the case B. The increase in calcareous pelagic production calculated by the model contrasts with the decrease in size and abundance of *Prinziosphera* observed in the late Rhaetian Austrian section from Kuhjoch and interpreted as successive acidification events (Clémence et al., 2010b).

The global biological productivity increase, due to an increase in phosphate weathering, is inconsistent with the paleontological observations and shows the limit of computing primary productivity as a function of phosphate delivery together with pelagic carbonate production as a function of primary productivity. In a biological crisis situation, species have different responses and in the case of the TJB crisis, calcareous organisms in epicontinental seas are affected and are supplanted by picoplankton or organic-walled organism (Clémence et al., 2010a,b; Paris et al., 2010; van de Schootbrugge et al., 2007). As a consequence, calcareous pelagic organisms might be influenced by saturation state variations in the same way as reef building organisms, reinforcing the carbonate production crisis observed in the late Rhaetian. The acidification observed in Austria events slightly predates the late Rhaetian carbon isotopes negative excursion. According to Marzoli et al. (2004), this is also the case for the onset of the CAMP in Morocco. As a consequence, late Rhaetian acidifications of Austrian basin, occurring prior to the first excursion (Clémence et al., 2010b) could be due to the early CAMP volcanic phase. Our results suggest that 0.15 pH decrease occurring in less than 200 yr alter reef productivity. The sedimentary record show that plankton is affected as well, so such peak of degassing and consequent oceanic acidification are likely to strongly perturb calcareous primary producers. Furthermore, short and strong perturbations of seawater chemistry are probably more likely to generate a biological crisis than moderate perturbation of seawater chemistry due to an evolution of the atmospheric CO<sub>2</sub> content on a scale of hundred thousand years. Succession of pulses

## Modeling the consequences on late Triassic environment

G. Paris et al.

Title Page

Abstract

Introduction

Conclusions

References

Tables

Figures

⏪

⏩

◀

▶

Back

Close

Full Screen / Esc

Printer-friendly Version

Interactive Discussion



could also affect successively different species, potentially explaining the dispersion of extinctions observed in available sections (Hesselbo et al., 2007).

Indeed, modeling a Gaussian carbon emission does not significantly perturb the carbon cycle at the TJB, even if a global atmospheric  $p\text{CO}_2$  increase is observed in our model. Over such a time span, oceanic  $\text{CO}_2$  remains in equilibrium with atmospheric  $\text{CO}_2$  and weathering fluxes counteract for atmospheric  $p\text{CO}_2$  increase in epicontinental seas. Indeed, the alkalinity delivered by weathering to epicontinental seas leads to an increase in the reef production. Due to mixing time, alkalinity cumulates in the epicontinental sea and counteracts for the pH diminution mirroring the atmospheric  $p\text{CO}_2$  increase. The main part of the carbonate production occurs in this epicontinental photic zone, neritic production increases as well (Fig. 4a). Epicontinental bottom waters (Fig. 4b) and open ocean epicontinental zone (Fig. 4c) are not the main place for carbonate factory in the late Triassic oceans. The only way to decrease the saturation state in the epicontinental photic zone is simulated by scenario B (Fig. 4a).

The simulated pulse-like degassing induces 15 ky lasting diminution of reef production with maximum diminution of 30%. Nevertheless, the underlying mechanism is not undersaturation in itself, rather a significant decrease in oceanic saturation state. Abrupt atmospheric  $p\text{CO}_2$  increase induces the formation of bicarbonate ion in seawater to the detriment of carbonate ions. Previous modeling results had contrasted conclusions concerning variations of the seawater saturation state, suggesting that undersaturation could be reached at the TJB for the entire ocean (Berner and Beerling, 2007). The required conditions to generate an undersaturation are 21 000 Gt C degassed by the CAMP, emitted onto the atmosphere in 100 kyr and a pre-perturbation saturation state fixed by the authors at a value of 1.1 (Berner and Beerling, 2007). The  $\text{CO}_2$  degassing is associated to huge amount of methane and  $\text{SO}_2$  delivered to the atmosphere. The considered values are lying in the upper range of independent estimates, as stated by the authors (Berner and Beerling, 2007).

Concerning the pre-crisis saturation state, the value in the present study is calculated with our geochemical box model. The calculated value is a saturation state of 2.1

## Modeling the consequences on late Triassic environment

G. Paris et al.

Title Page

Abstract

Introduction

Conclusions

References

Tables

Figures

⏪

⏩

◀

▶

Back

Close

Full Screen / Esc

Printer-friendly Version

Interactive Discussion

(compared to a modern value of 4), much higher than the 1.1 value (Berner and Beerling, 2007). This reinforces our main conclusion that Gaussian-like degassing is not the mechanism responsible for the carbonate production crisis and that undersaturation is not reached. This underlines the influence of pulse-like degassing at the TJB.

## 7 Conclusions

A carbonate production decrease is observed in the late Rhaetian, concomitant to a negative excursion in both  $\delta^{13}\text{C}_{\text{org}}$  and  $\delta^{13}\text{C}_{\text{min}}$  values and an increase in atmospheric  $p\text{CO}_2$ . The negative excursion is estimated to last for 200–500 kyr, consistent with estimate of the paroxysmal phase of CAMP emplacement duration. Three major points are taken out of this study. (1) To explore the consequences of LIP degassing on the paleoenvironment in a given geological context, not only the degassing scenario but also the paleogeography play a key role. Different part of the ocean will have different response. Paleocirculation in the Panthalassa would help to better constrain the consequences of atmospheric  $\text{CO}_2$  increase. (2) The response of biological pump to such environmental perturbation remains poorly understood at a large scale and is more complex than what can be taken into account in the model in its present form. (3) Clathrates might not be the only source for intense negative carbon isotope excursions in the geological past of Earth.

1. The CAMP emplacement occurred as intense pulses shorter than 400 yr (Knight et al., 2004). By modeling a degassing of ten pulses of 100 yr, we observe a succession of 30 % carbonate production decreases in contrast with the consequences of the traditionally used Gaussian-like degassing over the duration of the paroxysmal phase. This decrease occurs even if undersaturation is not reached in the ocean.
2. Break down of biological primary productivity can also account for part of the sedimentary carbon isotope excursions and for part of the atmospheric  $p\text{CO}_2$

## Modeling the consequences on late Triassic environment

G. Paris et al.

Title Page

Abstract

Introduction

Conclusions

References

Tables

Figures

⏪

⏩

◀

▶

Back

Close

Full Screen / Esc

Printer-friendly Version

Interactive Discussion



**Modeling the consequences on late Triassic environment**

G. Paris et al.

Title Page

Abstract

Introduction

Conclusions

References

Tables

Figures

◀

▶

◀

▶

Back

Close

Full Screen / Esc

Printer-friendly Version

Interactive Discussion



in this model. However, it is hard to quantify and does not allow reaching the expected level. The results of the present calculations emphasize the role played by intense volcanism on carbonate production but does not account for expected sulfur dioxide emissions that could lead to enhanced acidification of seawater, continental biomass poisoning (van de Schootbrugge et al., 2009) and potential cooling (Schoene et al., 2010). It shows however that a progressive degassing of CO<sub>2</sub> to the atmosphere over 500 ky is not able to alter the chemical composition of epicontinental seas in a way such that calcareous production is perturbed, in agreement with micropaleontological studies from Austria (Clémence et al., 2010b).

3. Nevertheless, this CAMP degassing scenario and associated present modeling fails to reproduce the observed negative  $\delta^{13}\text{C}$  excursion in the late Rhaetian sediments. At the present level of understanding of the carbon cycle, the most efficient way to mimic carbon isotope excursions linked to volcanic degassing during major environmental crises is obtained by adding carbon with a very low isotopic signature to the atmosphere. So far, this has been simulated by assuming methane degassing or a contribution of sedimentary organic carbon in metamorphic processes. Deines (2002) and Cartigny (2010) have inferred the existence of mantellic carbon with low isotopic composition and such marked isotopic signature may potentially come directly from the mantle. By assuming a  $-20\text{‰}$  isotopic composition for the CO<sub>2</sub> released by the CAMP, we reproduce the intensity of the first negative excursion in  $\delta^{13}\text{C}_{\text{org}}$  values. This is a speculative but interesting hypothesis which should be further explored, particularly to fix the allowed range of carbon isotope signature of mantle degassed carbon.

*Acknowledgements.* The authors thank Sébastien Nomade (LSCE) and Pierre Cartigny (IPGP) for fruitful discussions. We are grateful to Annachiara Bartolini (MNHN) for fruitful comments on earlier versions of the present article and her contribution for significant improvements to its quality. This work was granted through IFP-IPGP convention no. 31-231.

The publication of this article is financed by CNRS-INSU.

## References

- Beerling, D. and Berner, R.: Biogeochemical constraints on the Triassic-Jurassic boundary carbon cycle event, *Global Biogeochem. Cy.*, 16, 1029, doi:10.1029/2001GB001637, 2002.
- Berner, R. A. and Beerling, D. J.: Volcanic degassing necessary to produce a  $\text{CaCO}_3$  undersaturated ocean at the Triassic-Jurassic boundary, *Palaeogeogr. Palaeoclimatol.*, 244, 368–373, 2007.
- Cartigny, P.: Stable isotopes and the origin of diamond, *Elements*, 1, 79–84, doi:10.2113/gselements.1.2.79, 2005.
- Cartigny, P.: Mantle-related carbonados? Geochemical insights from diamonds from the Dacheine komatiite (French Guiana), *Earth Planet. Sc. Lett.*, 296, 329–339, 2010.
- Catubig, N. R., Archer, D. E., Francois, R., and DeMenocal, P.: Global deep-sea burial rate of calcium carbonate during the last glacial maximum, *Paleoclimatology*, 13, 298–310, 1998.
- Cirilli, S., Marzoli, A., Tanner, L., Bertrand, H., Buratti, N., Jourdan, F., Bellieni, G., Kontak, D., and Renne, P. R.: Latest Triassic onset of the Central Atlantic Magmatic Province (CAMP) volcanism in the Fundy Basin (Nova Scotia): New stratigraphic constraints, *Earth Planet. Sc. Lett.*, 286, 514–525, 2009.
- Chenet, A., Fluteau, F., Courtillot, V., Gerard, M., and Subbarao, K.: Determination of rapid Deccan eruptions across the KTB using paleomagnetic secular variation: (I) Results from 1200 m thick section in the Mahabaleshwar escarpment, *J. Geophys. Res.*, 113, B04101, doi:10.1029/2006JB004635, 2008.
- Chenet, A.-L., Courtillot, V., Fluteau, F., Gérard, M., Quidelleur, X., Khadri, S. F. R., Subbarao, K. V., and Thordarson, T.: Determination of rapid Deccan eruptions across the Cretaceous-Tertiary boundary using paleomagnetic secular variation: 2. Constraints from analysis of

## Modeling the consequences on late Triassic environment

G. Paris et al.

Title Page

Abstract

Introduction

Conclusions

References

Tables

Figures

⏪

⏩

◀

▶

Back

Close

Full Screen / Esc

Printer-friendly Version

Interactive Discussion

**Modeling the consequences on late Triassic environment**

G. Paris et al.

[Title Page](#)[Abstract](#)[Introduction](#)[Conclusions](#)[References](#)[Tables](#)[Figures](#)[⏪](#)[⏩](#)[◀](#)[▶](#)[Back](#)[Close](#)[Full Screen / Esc](#)[Printer-friendly Version](#)[Interactive Discussion](#)

eight new sections and synthesis for a 3500-m-thick composite section, *J. Geophys. Res.*, 114, B06103, doi:10.1029/2008jb005644, 2009.

Clémence, M.-E., Bartolini, A., Gardin, S., Paris, G., Beaumont, V., and Page, K. N.: Early Hettangian benthic-planktonic coupling at Doniford (SW England): Palaeoenvironmental implications for the aftermath of the end-Triassic crisis, *Palaeogeogr. Palaeoclimatol.*, 295, 102–115, 2010a.

Clémence, M.-E., Gardin, S., Bartolini, A., Paris, G., Beaumont, V., and Guex, J.: Benthic-planktonic evidence from the Austrian Alps for a decline in sea-surface carbonate production at the end of the Triassic, *Swiss J. Geosci.*, 103, 293–315, 2010b.

Courtillot, V.: Mass extinctions in the last 300 million years: One impact and seven flood basalts?, *Israel J. Earth Sci.*, 43, 255–266, 1994.

Courtillot, V., Besse, J., Vandamme, D., Montigny, R., Jaeger, J.-J., and Cappetta, H.: Deccan flood basalts at the Cretaceous/Tertiary boundary?, *Earth Planet. Sc. Lett.*, 80, 361–374, 1986.

Courtillot, V., Jaupart, C., Manighetti, I., Tapponnier, P., and Besse, J.: On causal links between flood basalts and continental breakup, *Earth Planet. Sc. Lett.*, 166, 177–195, 1999.

Deines, P.: The carbon isotope geochemistry of mantle xenoliths, *Earth-Sci. Rev.*, 58, 247–278, 2002.

Dessert, C., Dupré, B., François, L. M., Schott, J., Gaillardet, J., Chakrapani, G., and Bajpai, S.: Erosion of Deccan Traps determined by river geochemistry: impact on the global climate and the  $^{87}\text{Sr}/^{86}\text{Sr}$  ratio of seawater, *Earth Planet. Sc. Lett.*, 188, 459–474, 2001.

Dessert, C., Dupré, B., Gaillardet, J., François, L. M., and Allègre, C. J.: Basalt weathering laws and the impact of basalt weathering on the global carbon cycle, *Chem. Geol.*, 202, 257–273, 2003.

Donnadieu, Y., Goddérès, Y., Pierrehumbert, R., Dromart, G., Fluteau, F., and Jacob, R.: A GEOCLIM simulation of climatic and biogeochemical consequences of Pangea breakup, *Geochem. Geophys. Geosy.*, 7, Q11019, doi:10.1029/2006GC001278, 2006a.

Donnadieu, Y., Pierrehumbert, R., Jacob, R., and Fluteau, F.: Modelling the primary control of paleogeography on Cretaceous climate, *Earth Planet. Sc. Lett.*, 248, 426–437, 2006b.

François, L. M., Walker, J. C. G., and Opdyke, B. N.: The history of global weathering and the chemical evolution of the ocean-atmosphere system, *Evol. Earth Planets*, 14, 143–159, 1993.

**Modeling the consequences on late Triassic environment**

G. Paris et al.

[Title Page](#)[Abstract](#)[Introduction](#)[Conclusions](#)[References](#)[Tables](#)[Figures](#)[⏪](#)[⏩](#)[◀](#)[▶](#)[Back](#)[Close](#)[Full Screen / Esc](#)[Printer-friendly Version](#)[Interactive Discussion](#)

Gaillardet, J., Dupré, B., Louvat, P., and Allègre, C. J.: Global silicate weathering and CO<sub>2</sub> consumption rates deduced from the chemistry of large rivers, *Chem. Geol.*, 159, 3–30, 1999.

Galli, M. T., Jadoul, F., Bernasconi, S. M., and Weissert, H.: Anomalies in global carbon cycling and extinction at the Triassic/Jurassic boundary: evidence from a marine C-isotope record, *Palaeogeogr. Palaeoclimatol.*, 216, 203–214, 2005.

Goddéris, Y. and Joachimski, M. M.: Global change in the Late Devonian: modelling the Frasnian-Famennian short-term carbon isotope excursions, *Palaeogeogr. Palaeoclimatol.*, 202, 309–329, 2004.

Grard, A., Francois, L. M., Dessert, C., Dupre, B., and Godderis, Y.: Basaltic volcanism and mass extinction at the Permo-Triassic boundary: Environmental impact and modeling of the global carbon cycle, *Earth Planet. Sc. Lett.*, 234, 207–221, 2005.

Guex, J., Bartolini, A., Atudorei, V., and Taylor, D.: High-resolution ammonite and carbon isotope stratigraphy across the Triassic-Jurassic boundary at New York Canyon (Nevada), *Earth Planet. Sc. Lett.*, 225, 29–41, 2004.

Guidry, M. W. and Mackenzie, F. T.: Experimental study of igneous and sedimentary apatite dissolution: Control of pH, distance from equilibrium, and temperature on dissolution rates, *Geochim. Cosmochim. Acta*, 67, 2949–2963, 2003.

Hayes, J. M., Strauss, H., and Kaufman, A. J.: The abundance of <sup>13</sup>C in marine organic matter and isotopic fractionation in the global biogeochemical cycle of carbon during the past 800 Ma, *Chem. Geol.*, 161, 103–125, 1999.

Hesselbo, S., Robinson, S., Surlyk, F., and Piasecki, S.: Terrestrial and marine extinction at the Triassic-Jurassic boundary synchronized with major carbon-cycle perturbation: A link to initiation of massive volcanism?, *Geology*, 30, 251–254, 2002.

Hesselbo, S. P., McRoberts, C. A., and Pálffy, J.: Triassic-Jurassic boundary events: Problems, progress, possibilities, *Palaeogeogr. Palaeoclimatol.*, 244, 1–10, 2007.

Huynh, T. T. and Poulsen, C. J.: Rising atmospheric CO<sub>2</sub> as a possible trigger for the end-Triassic mass extinction, *Palaeogeogr. Palaeoclimatol.*, 217, 223–242, 2005.

Knight, K. B., Nomade, S., Renne, P. R., Marzoli, A., Bertrand, H., and Youbi, N.: The Central Atlantic Magmatic Province at the Triassic-Jurassic boundary: paleomagnetic and <sup>40</sup>Ar/<sup>39</sup>Ar evidence from Morocco for brief, episodic volcanism, *Earth Planet. Sc. Lett.*, 228, 143–160, 2004.

## Modeling the consequences on late Triassic environment

G. Paris et al.

Title Page

Abstract

Introduction

Conclusions

References

Tables

Figures

◀

▶

◀

▶

Back

Close

Full Screen / Esc

Printer-friendly Version

Interactive Discussion



Kürschner, W. M., Bonis, N. R., and Krystyn, L.: Carbon-isotope stratigraphy and palynostratigraphy of the Triassic-Jurassic transition in the Tiefengraben section – Northern Calcareous Alps (Austria), *Palaeogeogr. Palaeoclimatol.*, 244, 257–280, 2007.

Li, S. L., Calmels, D., Han, G., Gaillardet, J., and Liu, C. Q.: Sulfuric acid as an agent of carbonate weathering constrained by  $^{13}\text{C}_{\text{DIC}}$ : Examples from Southwest China, *Earth Planet. Sc. Lett.*, 270, 189–199, 2008.

Mankinen, E. A., Prévôt, M., Grommé, C. S., and Ní, R.S.: The Steens Mountain (Oregon) geomagnetic polarity transition 1. Directional history, duration of episodes, and rock magnetism, *J. Geophys. Res.*, 90, 10393–10416, 1985.

Marzoli, A., Renne, P., Piccirillo, E., Ernesto, M., Bellieni, G., and De Min, A.: Extensive 200-Million-Year-Old Continental Flood Basalts of the Central Atlantic Magmatic Province, *Science*, 284, 616–618, 1999.

Marzoli, A., Bertrand, H., Knight, K., Cirilli, S., Buratti, N., Verati, C., Nomade, S., Renne, P., Youbi, N., and Martini, R.: Synchrony of the Central Atlantic magmatic province and the Triassic-Jurassic boundary climatic and biotic crisis, *Geology*, 32, 973–976, 2004.

Marzoli, A., Bertrand, H., Knight, K. B., Cirilli, S., Nomade, S., Renne, P. R., Verati, C., Youbi, N., Martini, R., and Bellieni, G.: Comment on “Synchrony between the Central Atlantic magmatic province and the Triassic-Jurassic mass-extinction event? By Whiteside et al. (2007)”, *Palaeogeogr. Palaeoclimatol.*, 262, 189–193, 2008.

McElwain, J. C., Wagner, F., Kürschner, W. M., and van Bergen, P. F.: Do Fossil Plants Signal Palaeoatmospheric  $\text{CO}_2$  Concentration in the Geological Past? [and Discussion], *Philos. T. Biol. Sci.*, 353, 83–96, 1998.

McElwain, J. C., Beerling, D. J., and Woodward, F. I.: Fossil Plants and Global Warming at the Triassic-Jurassic Boundary, *Science*, 285, 1386–1390, 1999.

McElwain, J. C., Wagner, P. J., and Hesselbo, S. P.: Fossil Plant Relative Abundances Indicate Sudden Loss of Late Triassic Biodiversity in East Greenland, *Science*, 324, 1554–1556, doi:10.1126/science.1171706, 2009.

McHone, J. G.: Non-plume magmatism and rifting during the opening of the central Atlantic Ocean, *Tectonophysics*, 316, 287–296, 2000.

McHone, J. G.: Volatile Emissions from Central Atlantic Magmatic Province basalts: mass assumptions and environmental consequences, in: *The Central Atlantic Magmatic Province: insights from fragments of Pangea*, edited by: Hames, J. G. M., Renne, P., and Ruppel, C., *Geophysical Monography Series*, AGU, Washington, D.C., 241–254, 2002.

## Modeling the consequences on late Triassic environment

G. Paris et al.

Title Page

Abstract

Introduction

Conclusions

References

Tables

Figures

◀

▶

◀

▶

Back

Close

Full Screen / Esc

Printer-friendly Version

Interactive Discussion



Moulin, M., Fluteau, F., Courtillot, V., Marsh, J., Delpéché, G., Quidelleur, X., Gérard, M., and Jay, A. E.: An attempt to constrain the age, duration, and eruptive history of the Kaaroo flood basalt: Naude's Nek section (South Africa), *J. Geophys. Res.*, 116, B07403, doi:10.1029/2011jb008210, 2011.

5 Nomade, S., Knight, K., Beutel, E., Renne, P., Verati, C., Féraud, G., Marzoli, A., Youbi, N., and Bertrand, H.: Chronology of the Central Atlantic Magmatic Province: Implications for the Central Atlantic rifting processes and the Triassic-Jurassic biotic crisis, *Palaeogeogr. Palaeoclimatol.*, 244, 326–344, 2007.

10 Oliva, P., Viers, J., and Dupré, B.: Chemical weathering in granitic environments, *Chem. Geol.*, 202, 225–256, 2003.

Olsen, P. E., Schlische, R. W., and Fedosh, M. S.: 580 ky duration of the Early Jurassic flood basalt event in eastern North America estimated using Milankovitch cyclostratigraphy, *The continental Jurassic: Museum of Northern Arizona Bulletin*, 60, 11–22, 1996.

15 Opdyke, B. N. and Wilkinson, B. H.: Carbonate mineral saturation state and cratonic limestone accumulation, *Am. J. Sci.*, 293, 217–234, 1993.

Pagani, M., Freeman, K. H., and Arthur, M. A.: Late Miocene Atmospheric CO<sub>2</sub> Concentrations and the Expansion of C<sub>4</sub> Grasses, *Science*, 285,, 876–879, doi:10.1126/science.285.5429.876, 1999.

20 Pálfy, J., Demeny, A., Haas, J., Hetenyi, M., Orchard, M., and Veto, I.: Carbon isotope anomaly and other geochemical changes at the Triassic-Jurassic boundary from a marine section in Hungary, *Geology*, 29, 1047–1050, 2001.

Paris, G., Beaumont, V., Bartolini, A., Clémence, M., Gardin, S., and Page, K.: Nitrogen isotope record of a perturbed paleoecosystem in the aftermath of the end-Triassic crisis, Doniford section, SW England, *Geochem. Geophys. Geosyst.*, 11, Q08021, doi:10.1029/2010GC003161, 2010.

25 Prévot, M. and McWilliams, M.: Paleomagnetic correlation of Newark Supergroup volcanics, *Geology*, 17, 1007–1010, 1989.

Riisager, J., Riisager, P., and Pedersen, A. K.: Paleomagnetism of large igneous provinces: case-study from West Greenland, North Atlantic igneous province, *Earth Planet. Sc. Lett.*, 214, 409–425, 2003.

30 Riisager, P., Riisager, J., Abrahamsen, N., and Waagstein, R.: New paleomagnetic pole and magnetostratigraphy of Faroe Islands flood volcanics, North Atlantic igneous province, *Earth Planet. Sc. Lett.*, 201, 261–276, 2002.

- Rowley, D. B.: Rate of plate creation and destruction: 180 Ma to present, *Bull. Geol. Soc. Am.*, 114, 927–933, 2002.
- Ruhl, M., Kürschner, W. M., and Krystyn, L.: Triassic-Jurassic organic carbon isotope stratigraphy of key sections in the western Tethys realm (Austria), *Earth Planet. Sc. Lett.*, 281, 169–187, 2009.
- 5 Sarmiento, J. L., Orr, J. C., and Siegenthaler, U.: A Perturbation Simulation of CO<sub>2</sub> Uptake in an Ocean General Circulation Model, *J. Geophys. Res.*, 97, 3621–3645, 1992.
- Schaller, M. F., Wright, J. D., and Kent, D. V.: Atmospheric pCO<sub>2</sub> Perturbations Associated with the Central Atlantic Magmatic Province, *Science*, 331, 1404–1409, doi:10.1126/science.1199011, 2011.
- 10 Schaltegger, U., Guex, J., Bartolini, A., Schoene, B., and Ovtcharova, M.: Precise U-Pb age constraints for end-Triassic mass extinction, its correlation to volcanism and Hettangian post-extinction recovery, *Earth Planet. Sci. Lett.*, 267, 266–275, 2007.
- Schoene, B., Guex, J., Bartolini, A., Schaltegger, U., Blackburn, T. J., and Bowring, S. A.: Correlating the end-Triassic mass extinction and flood basalt volcanism at the 100 ka level, *Geology*, 38, 387–390, 2010.
- 15 Sepkoski, J. J.: Patterns of Phanerozoic extinction: a perspective from global data bases, in: *Global events and event stratigraphy*, Springer, Berlin, 35–52, 1996.
- Simon, L., Godd eris, Y., Werner, B., Strauss, H., and Joachimski, M. M.: Modeling the carbon and sulfur isotope compositions of marine sediments: Climate evolution during the Devonian, *Chem. Geol.*, 246, 19–38, 2007.
- 20 van de Schootbrugge, B., Tremolada, F., Rosenthal, Y., Bailey, T. R., Feist-Burkhardt, S., Brinkhuis, H., Pross, J., Kent, D. V., and Falkowski, P. G.: End-Triassic calcification crisis and blooms of organic-walled “disaster species”, *Palaeogeogr. Palaeoclimatol.*, 244, 126–141, 2007.
- 25 van de Schootbrugge, B., Payne, J. L., Tomasovych, A., Pross, J., Fiebig, J., Benbrahim, M., F llmi, K. B., and Quan, T. M.: Carbon cycle perturbation and stabilization in the wake of the Triassic-Jurassic boundary mass-extinction event, *Geochem. Geophys. Geosyst.*, 9, Q04028, doi:10.1029/2007GC001914, 2008.
- van de Schootbrugge, B., Quan, T. M., Lindstr m, S., P ttmann, W., Heunisch, C., Pross, J., Fiebig, J., Petschick, R., R hling, H. G., and Richoz, S.: Floral changes across the Triassic/Jurassic boundary linked to flood basalt volcanism, *Nat. Geosci.*, 2, 589–594, 2009.
- 30 Vogt, P. R.: Evidence for global synchronism in mantle plume convection, and possible significance for geology, *Nature*, 240, 338–342, 1972.

## Modeling the consequences on late Triassic environment

G. Paris et al.

[Title Page](#)[Abstract](#)[Introduction](#)[Conclusions](#)[References](#)[Tables](#)[Figures](#)[⏪](#)[⏩](#)[◀](#)[▶](#)[Back](#)[Close](#)[Full Screen / Esc](#)[Printer-friendly Version](#)[Interactive Discussion](#)

**Modeling the  
consequences on  
late Triassic  
environment**

G. Paris et al.

[Title Page](#)[Abstract](#)[Introduction](#)[Conclusions](#)[References](#)[Tables](#)[Figures](#)[⏪](#)[⏩](#)[◀](#)[▶](#)[Back](#)[Close](#)[Full Screen / Esc](#)[Printer-friendly Version](#)[Interactive Discussion](#)

Walker, L. J., Wilkinson, B. H., and Ivany, L. C.: Continental drift and Phanerozoic carbonate accumulation in shallow-shelf and deep-marine settings, *J. Geol.*, 110, 75–87, 2002.

Ward, P. D., Haggart, J. W., Carter, E. S., Wilbur, D. O., Tipper, H. W., and Evans, T.: Sudden Productivity Collapse Associated with the Triassic-Jurassic Boundary Mass Extinction, *Science*, 292, 1148–1151, 2001.

Whiteside, J. H., Olsen, P. E., Kent, D. V., Fowell, S. J., and Et-Touhami, M.: Synchrony between the Central Atlantic magmatic province and the Triassic-Jurassic mass-extinction event?, *Palaeogeogr. Palaeoclimatol.*, 244, 345–367, 2007.

Whiteside, J. H., Olsen, P. E., Eglinton, T., Brookfield, M. E., and Sambrotto, R. N.: Compound-specific carbon isotopes from Earth's largest flood basalt eruptions directly linked to the end-Triassic mass extinction, *P. Natl. Acad. Sci.*, 107 6721, doi:10.1073/pnas.1001706107, 2010.

## Modeling the consequences on late Triassic environment

G. Paris et al.

**Table 1.** Estimations of the CO<sub>2</sub> volume emitted by the CAMP.

	Basalt volume (km <sup>3</sup> )	CO <sub>2</sub> content % wt	% degassed CO <sub>2</sub>	Gt CO <sub>2</sub>	Gt C
McHone (2002) low hypothesis	$2.385 \times 10^6$	0.117	70 %	5200	1420
Olsen (1999) high hypothesis	$8 \times 10^6$	0.6	100 %*	128 000	34 910

\* Estimation of Beerling and Berner (2002).

Title Page

Abstract

Introduction

Conclusions

References

Tables

Figures

◀

▶

◀

▶

Back

Close

Full Screen / Esc

Printer-friendly Version

Interactive Discussion



## Modeling the consequences on late Triassic environment

G. Paris et al.

**Table 2.** Equations describing the carbon cycle used in the model with  $K_0$  constant,  $p\text{CO}_2^{\text{atm}}$  the atmospheric  $p\text{CO}_2$  (partial pressure of  $\text{CO}_2$ ),  $p\text{CO}_2^j$  the dissolved  $p\text{CO}_2$  in reservoir  $j$ ,  $R$  the perfect gas constant,  $E_a^{\text{silw}}$ ,  $E_a^{\text{basw}}$  and  $E_a^{\text{pw}}$  the apparent activation energy of granite (48 200 J mol<sup>-1</sup>), basalt (42 300 J mol<sup>-1</sup>) and phosphorite (34 777 J mol<sup>-1</sup>) weathering, respectively.  $n_{\text{pixel}}$  is the number of continental grid cells,  $\text{area}(i)$  is the surface of the continental grid cell  $i$ ,  $T(i)$  and  $\text{run}(i)$  are respectively the mean annual ground air temperature and the mean annual runoff for grid cell  $i$ . The number of superficial oceanic reservoir is  $n_{\text{reservoir}}$  and  $\text{surf}(j)$  represents the oceanic reservoir surface of the grid  $j$ .  $H_{\text{soil},i}$  is the proton concentration in soil solution for pixel  $i$ ,  $[\text{Ca}^{2+}]_{\text{eq}}$ : the calcium concentration within a solution soil calculated for each time step and for each pixel  $i$ . For neritic carbonate production,  $A_{\text{platform}}$  is the shelf platform area occupied by platform carbonate,  $\Omega_{\text{ara}}$  the aragonite solubility ratio and  $k_{\text{cr}}$  a calibration constant.

Air-sea $\text{CO}_2$ flux	$F_{\text{atm}} = \sum_{j=1}^{n_{\text{reservoir}}} K_0 \cdot (p\text{CO}_2^{\text{atm}} - p\text{CO}_2^j) \cdot \text{surf}(j).$	Sarmiento et al. (1992)
$\text{CO}_2$ consumption – granite weathering	$F_{\text{silw}} = \sum_{i=1}^{n_{\text{pixel}}} k_{\text{silw}} \cdot \text{run}(i) \cdot \text{area}(i) \cdot \exp \left[ \frac{E_a^{\text{silw}}}{R} \left( \frac{1}{T(i)} - \frac{1}{T_0} \right) \right]$	Oliva et al. (2003)
$\text{CO}_2$ consumption – basalt weathering	$F_{\text{basw}} = \sum_{i=1}^{n_{\text{pixel}}} k_{\text{basw}} \cdot \text{run}(i) \cdot \text{area}(i) \cot \exp \left[ \frac{E_a^{\text{basw}}}{R} \left( \frac{1}{T(i)} - \frac{1}{T_0} \right) \right]$	Dessert et al. (2001)
Phosphate weathering	$F_{\text{pw}} = \sum_{i=1}^{n_{\text{pixel}}} k_{\text{pw}} \cdot \text{run}(i) \cdot \text{area}(i) \cdot \exp \left[ \frac{E_a^{\text{pw}}}{R \cdot T(i)} \right] \cdot H_{\text{soil},i}^{0.27}$	Derived from Guidry and Mackenzie (2003)
Carbonate weathering	$F_{\text{cw}} = \sum_{i=1}^{n_{\text{pixel}}} k_{\text{cw}} \cdot \text{run}(i) \cdot \text{area}(i) \cdot [\text{Ca}^{2+}]_{\text{eq}}$	
Neritic carbonate flux	$F_{\text{neritic}} = k_{\text{cr}} \cdot A_{\text{platform}} \cdot (\Omega_{\text{ara}} - 1)^{1.7}$	Opdyke and Wilkinson (1993)

Title Page

Abstract

Introduction

Conclusions

References

Tables

Figures

◀

▶

◀

▶

Back

Close

Full Screen / Esc

Printer-friendly Version

Interactive Discussion



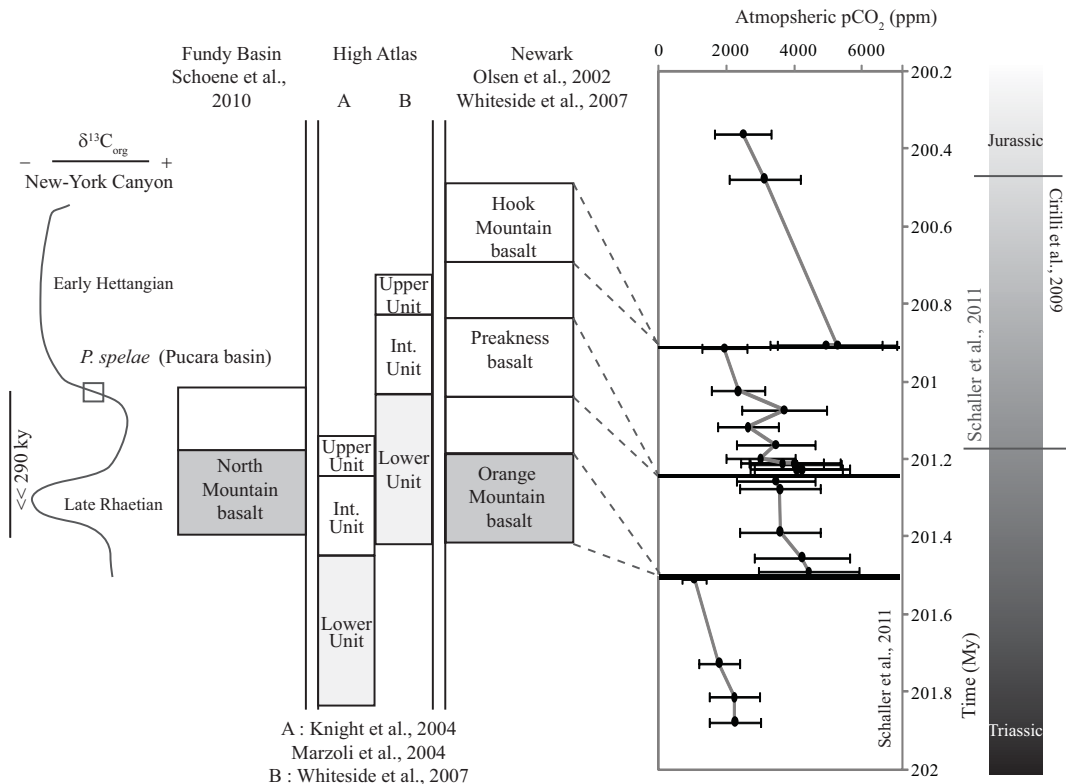


**Fig. 1.** Synchronicity between the late Rhaetian-early Hettangian sedimentary organic carbon isotopic composition negative excursion CAMP floodings from North America and Morocco, and Triassic-Jurassic boundary. Synchronicity between CAMP flooding and the New-York Canyon basin  $\delta^{13}\text{C}_{\text{org}}$  signal comes from Schoene et al. (2010) with the TJB being defined as first occurrence of *Psiloceras spelae* in the Pucara basin (Peru). The TJB position from Schaller et al. (2011) is based on palynological data from the Newark basin and the TJB position from Cirilli et al. (2009) is based on palynological assemblages from the Fundy basin.

## Modeling the consequences on late Triassic environment

G. Paris et al.

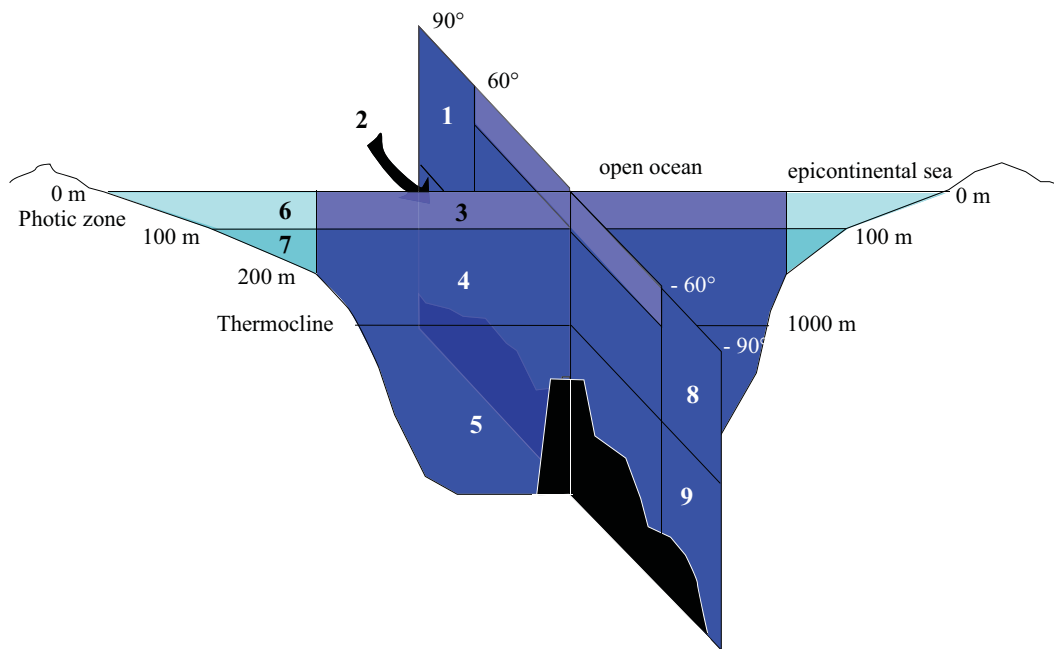


**Fig. 2.** Geometry of oceanic boxes used in the GEOCLIM model.

Title Page

Abstract

Introduction

Conclusions

References

Tables

Figures

◀

▶

◀

▶

Back

Close

Full Screen / Esc

Printer-friendly Version

Interactive Discussion

## Modeling the consequences on late Triassic environment

G. Paris et al.

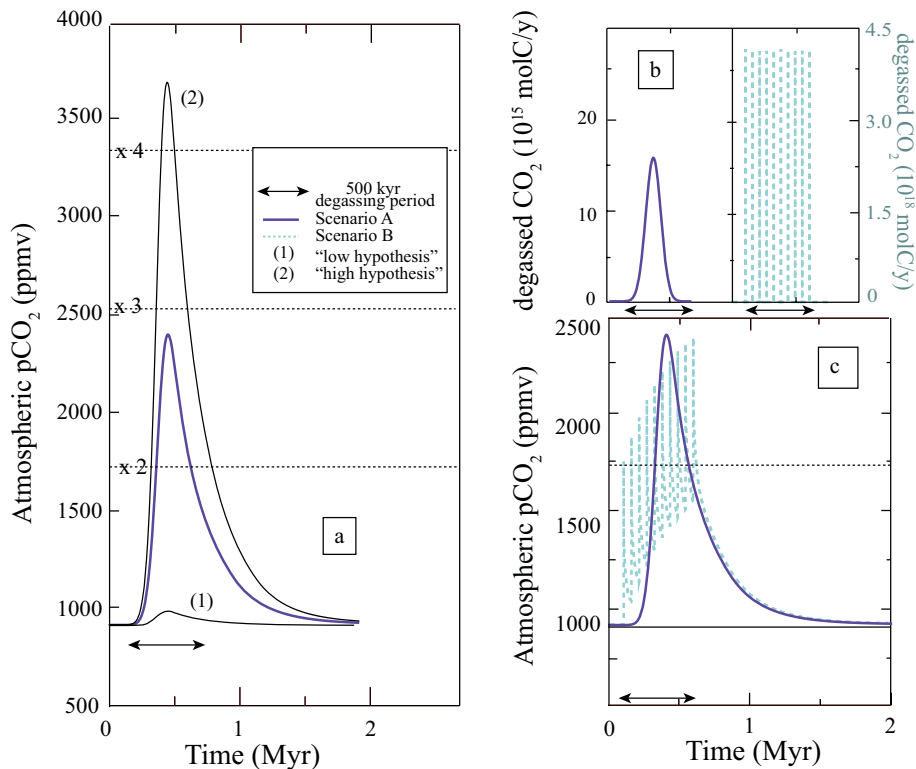


**Fig. 3.** (a) Calculated atmospheric  $p\text{CO}_2$ . The first peak (1) corresponds to the lowest volume of Table 1 (1440 Gt C) and (2) corresponds to the highest volume possible (34 290 Gt C). An intermediate volume 21 220 Gt C (scenario A) emitted fits the  $\text{CO}_2$  emission calculated by Beerling and Berner (2002) and is the total flux used for scenarios A and B (Fig. 3b). (b) Scenario A is a Gaussian flux, Scenario B consists in ten identical pulses. (c) Atmospheric  $p\text{CO}_2$  evolution according to the scenarios A and B. Dotted lines indicate atmospheric  $p\text{CO}_2$  proportional increase.

Title Page

Abstract

Introduction

Conclusions

References

Tables

Figures

◀

▶

◀

▶

Back

Close

Full Screen / Esc

Printer-friendly Version

Interactive Discussion

## Modeling the consequences on late Triassic environment

G. Paris et al.

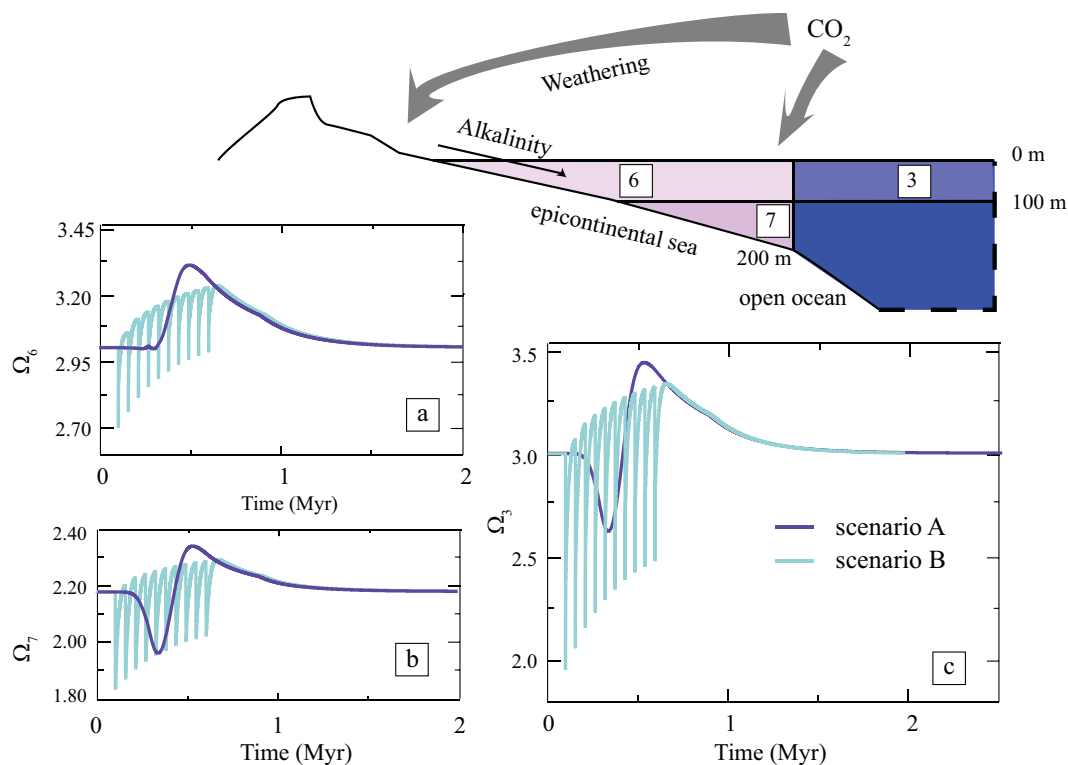


**Fig. 4.** Saturation state evolution of the epicontinental sea photic zone – oceanic box 6, **(a)** – and bottom waters – oceanic box 7, **(b)** – and of the open ocean photic zone – oceanic box 3, **(c)**. The CO<sub>2</sub> increase affects the continental weathering and the subsequent alkalinity delivering fluxes to the surface epicontinental waters.

Title Page

Abstract

Introduction

Conclusions

References

Tables

Figures

◀

▶

◀

▶

Back

Close

Full Screen / Esc

Printer-friendly Version

Interactive Discussion

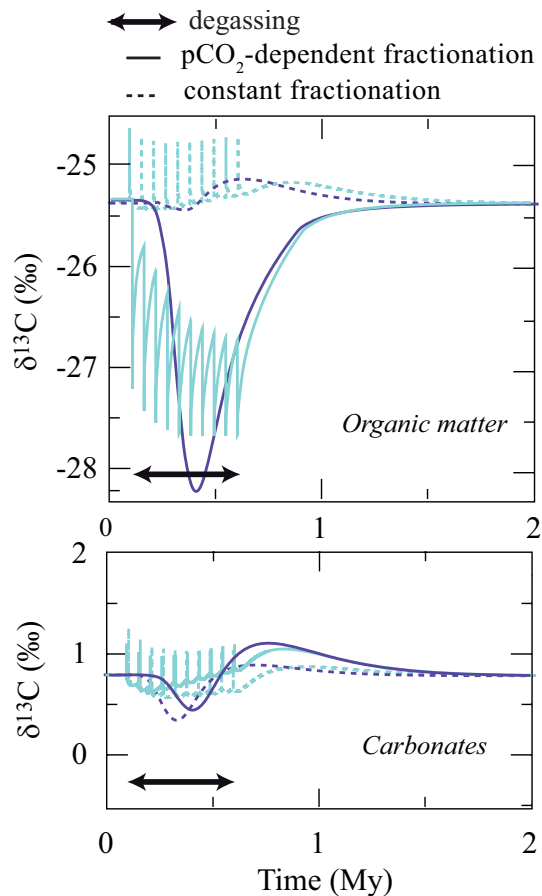


**Fig. 5.** Influence of the isotopic composition of the  $\text{CO}_2$  emitted by the CAMP for both scenarios A (dark curves) and B (light curves) in organic matter, atmosphere or carbonates. The  $p\text{CO}_2$  dependent fractionation is calculated according to Eq. (1) (solid line) or is constant.

## Modeling the consequences on late Triassic environment

G. Paris et al.

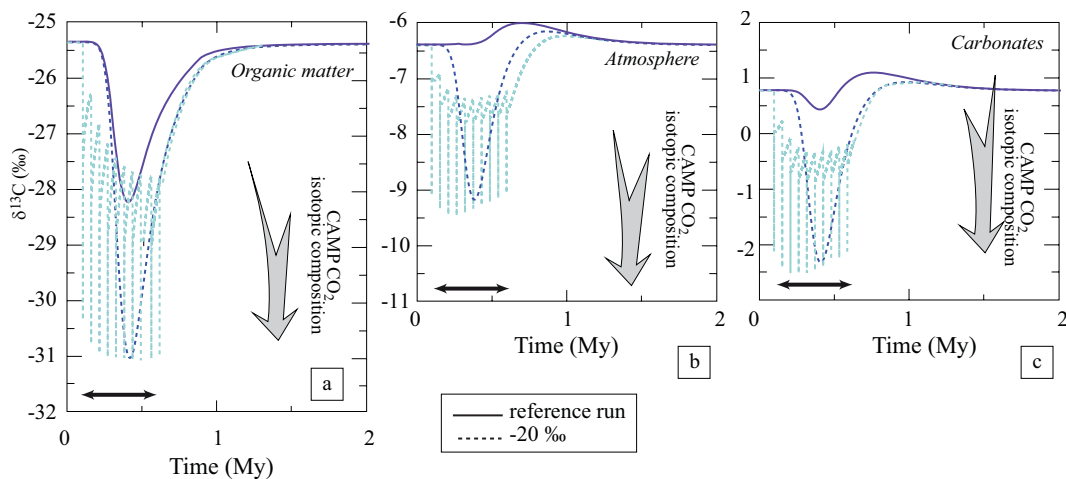


**Fig. 6.** Influence of the isotopic composition of the CO<sub>2</sub> emitted by the CAMP for both scenario A (dark curve) and B (light curve) for both organic matter (a), atmosphere (b) and carbonates (c).

Title Page

Abstract

Introduction

Conclusions

References

Tables

Figures

◀

▶

◀

▶

Back

Close

Full Screen / Esc

Printer-friendly Version

Interactive Discussion

## Modeling the consequences on late Triassic environment

G. Paris et al.

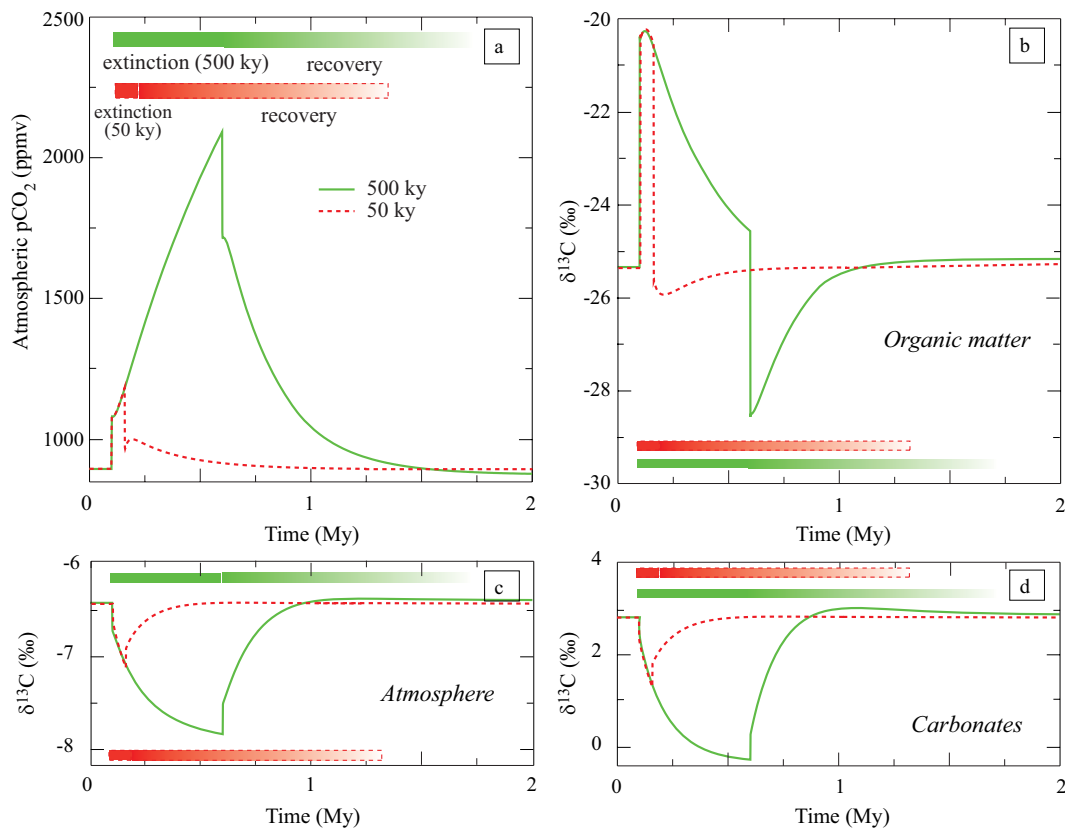


**Fig. 7.** Influence of biological productivity shutdown and following recovery on atmospheric  $p\text{CO}_2$  (a) and  $\delta^{13}\text{C}$  values of organic matter (b), atmosphere (c) and carbonates (d). Solid lines are for the 500 kyr shutdown and dot lines for the 50 kyr shutdown. Duration of biological productivity shutdown and following recovery for 50 kyr (red) and 500 kyr (green) are reminded in each sketch.